*Journal of
Nanoscience and Nanotechnology*
Vol. 8, 1–6, 2007

Ultralong Aligned Multi-Walled Carbon Nanotube for Electrochemical Sensing

Niramol Punbusayakul[1, 2, *], Lijie Ci[2], Saikat Talapatra[3], Werasak Surareungchai[1], and Pulickel M. Ajayan[2]

[1] *School of Bioresources and Technology, King Mongkut's University of Technology Thonburi,
Bangkhuntien-Chaitalay Rd., Thakam, Bangkok, 10150, Thailand*
[2] *Department of Materials Science and Engineering, Rensselaer Polytechnic Institute, Troy, NY 12180, USA*
[3] *Department of Physics, Southern Illinois University Carbondale, Carbondale, IL 62901, USA*

We have investigated electrochemical sensing properties of electrodes fabricated with ultralong aligned multi-walled carbon nanotube (MWNT) bundles synthesized using water-assisted chemical vapor deposition on aluminum (Al) and iron (Fe) coated silicon wafer with ethylene and argon/hydrogen gas as carbon source and buffer gas respectively. Cyclic voltammogram performed on these electrodes show diffusion-controlled-reversible reaction. The dominance of radial diffusion mass transport at these electrodes was also indicated by sigmoidal-shaped voltammograms obtained at various scan rates. These electrodes were able to sense very low concentration of ascorbic acid (~0.7 μM) and dopamine (~1.87 μM), two model species often used in electroanalysis. The excellent electrochemical properties along with good single species detection ability suggest that these MWNTs are promising electrode materials for developing very sensitive chemical and/or biological sensors.

Keywords: Multi-Walled Carbon Nanotubes, Electrochemical Sensing.

1. INTRODUCTION

Since their discovery, carbon nanotubes (CNTs) are envisioned as novel materials for various applications ranging from gas storage to components for nanoelectronic devices.[1–4] With properties such as large specific surface area, high thermal, mechanical and chemical stability, ability to accumulate analyte and minimum surface fouling effects they hold promise for potential materials for diverse electrochemical applications. As a result, a lot of investigations have focused on developing CNTs as a potential tool for many electrochemical applications such as biosensors and chemical sensors.[5–8] However, most of these studies were performed on macro architectures of CNTs electrodes.[9–13] In general, the major disadvantages of macroelectrode used for electrochemical sensing are the Ohmic drop and the presence of double layer capacitance (which leads to a distorted voltammogram).[14–16] The reduction of the size of the electrode overcomes these obstacles and also enhances electron transfer and mass transport at the working electrode surface. The smaller size of the electrodes also make them suitable for sensing very low concentrations of analyte species, even in low conductive media. The size reduction also leads to high current density and signal-to-noise ratio reduction.[14–16] This also holds true for CNTs electrodes. Therefore, it is essential to fabricate microelectrodes using CNTs to have electrochemical devices with better operating capabilities. In this article we present the electrochemical properties and sensing abilities of microelectrodes of ultralong multi-walled carbon nanotube bundles. These electrodes show a very wide window of working potential and were able to detect very low concentrations of ascorbic acid (AA) and dopamine (DA) concentrations as low as 0.7 and 1.87 μM respectively.

2. EXPERIMENTAL DETAILS

2.1. Multi-Walled Nanotubes (MWNTs) Synthesis

Vertically aligned-MWNT films were prepared by water-assisted chemical vapor deposition (CVD) process. Typically, an aluminum (Al) and iron (Fe) layer with 10 and 1–3 nm thickness respectively were deposited by e-beam deposition on the surface of a silicon wafer covered by a 1 μm thick silicon dioxide (SiO_2) layer. Ethylene was

---

[*] Author to whom correspondence should be addressed.

1533-4880/2007/8/001/006

doi:10.1166/jnn.2007.060

used as carbon source and argon (Ar)/hydrogen (H_2) (15% hydrogen content) as a buffer gas. In a typical CVD run, Ar/H_2 was flowed at the flow rate of 300 sccm through the alumina tube while the furnace was heated up to a temperature of 750–800 °C which allows for CNTs growth. After the furnace reached the set temperature, the Ar/H_2 flow rate was immediately increased to 1300 sccm and another portion of Ar/H_2 gas was flowed through a water bottle which was kept at room temperature, at a flow rate of 80 sccm, with ethylene gas being passed into the gas mixture with the flow rate of 100 sccm. The CNTs growth lasted for approximately 20 to 30 minutes. Once completed, the furnace was cooled down to room temperature under Ar/H_2 protection resulting in MWNT 'forest' ranging from 200 μm to several mm thick, with the MWNT average outer diameter of ~8 nm, as revealed from transmission electron microscopy (TEM) observation.

2.2. MWNTs Electrode Fabrication

For fabricating the electrodes, aligned-MWNT bundles were peeled off from the MWNT forest and placed on a flat glass substrate. One end of the bundles was subsequently attached to an electrical lead using conducting silver paste and the other end was fixed with epoxy glue for ease of handling of the electrode. Structural characterization of the electrodes was performed using field emission scanning electron microscopy (FESEM) and transmission electron microscopy (TEM).

2.3. Electrochemical Characterization

All the reagents used for the electrochemical measurements were of analytical grade, purchased from Sigma-Aldrich, except 5-hydroxytyramine hydrochloride (or dopamine; DA) was purchased from Fluka. Stock solutions of tested species, AA and DA, were freshly prepared in a phosphate buffer solution (PBS) (pH = 7.0). The buffer solutions and supporting electrolyte solutions were prepared in deionized water. The electrochemical properties of the electrodes were investigated in the standard three-electrode system, using a platinum wire as a counter electrode (CE) and silver/silver chloride (Ag/AgCl) as a reference electrode (RE). Cyclic voltammetry measurements were performed at room temperature in 10 mM potassium ferricyanide ($K_3Fe(CN)_6$) containing 0.1 M potassium chloride (KCl) solution, with various scan rates set by a potentiostat-galvanostat PAR 273A with the PowerSuite® data acquisition software.

3. RESULTS AND DISCUSSION

3.1. Electrochemical Characterization

In Figure 1 we have presented the nanotube material used in this study along with our data on electrochemical characterization of these electrodes. Figure 1(a) illustrates a typical FESEM image of aligned-MWNT forest. In Figure 1(b) TEM image of MWNTs are presented. A high resolution TEM image showing clean MWNT with well graphitized walls is shown in Figure 1(c). Figure 1(d) shows a cyclic voltammogram (CV) at the MWNT electrode in 0.1 M KCl solution at a scan rate of 20 mV/s. From the CV it is clear that there is no oxidation or reduction peaks at the MWNT electrode from potential ranging from −1.5 to 1.2 V. Consequently, a large window of working potential is available which allows for variation of the MWNT electrode in electroanalytical fields where it can donate and accept electrons over a wider range of potentials. This is very advantageous for certain high or extremely overpotential species. This also indicates that they can be used as a mediator in biosensor systems.[17]

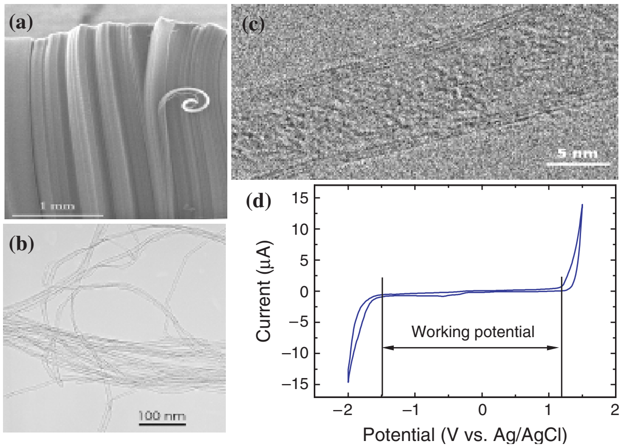

Fig. 1. (a) FESEM image of the as grown vertically aligned MWNT, (b) TEM image of MWNT, (c) HETEM image of MWNT illustrating the outer diameter of ~8 nm of the long MWNT, (d) CV at the MWNT microelectrode in 0.1 M KCl at the scan rate of 20 mVs.

Well-defined CVs with the increasing peak to peak separation (ΔEp) in 10 mM $K_3(Fe(CN)_6)$ containing 0.1 M KCl solution at the MWNT electrodes at various scan rates (5, 10, 20, 50, 100, 200 and 500 mV/s) are shown in Figure 2(a). An interesting phenomenon was observed during cyclic voltammetry performed with the same electrode after taking it out from the electrochemical cell and letting it dry under normal conditions. The voltammograms showed that with each subsequent drying process the CVs tend to acquire more and more S-shape or sigmoidal curve feature, though ΔEp remains stable. As shown in Figure 2(b) the CV signals tend to shrink from that shown in Figure 1(a). The data shown in Figure 2(b) was obtained after two sets of measurements and subsequent drying of the electrode. Figure 2(c) illustrates CVs obtained (with a scan rate of 5 mV/s) on the same MWNT electrode after consecutive voltammetry measurement and subsequent drying process. Most of the electrodes fabricated and tested showed this kind of behavior with very stable sigmoidal-shaped CV after few experimental runs

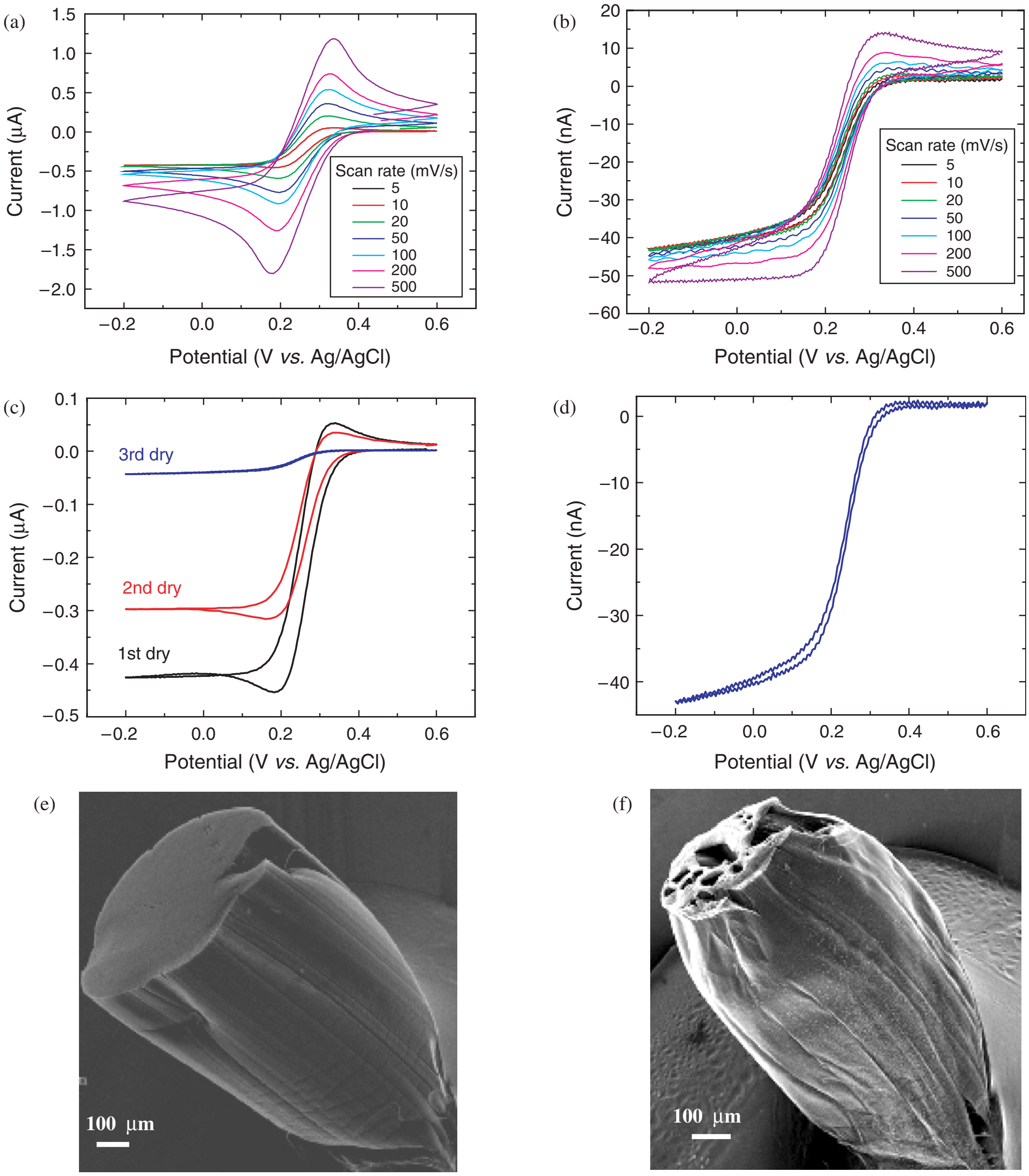

Fig. 2. (a) CVs of the MWNTs electrode in 10 mM $K_3(Fe(CN)_6$ containing 0.1 M KCl at 5, 10, 20, 50, 100, 200, and 500 mV/s from inner to outer loop respectively, (b) CVs on the same MWNT electrode after two cycles of measurement and drying cycle, (c) Comparison of the CVs from the MWNT electrode after various measurement and drying cycles performed at a scan rate of 5 mV/s. (d) Steady-state CV (signifying a microelectrode characteristic) after third measurement and drying cycle. (e) and (f) SEM images of an unfixed-end cylindrical electrode showing electrode compaction due to solvent evaporation.

and drying cycles. One such CV is shown in Figure 2(d). A possible reason for this could be the compaction of the MWNT bundles (see Figs. 2(e and f)) due to capillary forces acting on the CNTs which arises because of the solvent evaporation each time the electrodes were taken out of the electrochemical cell.[18–20] Typical volume filling fraction of our nanotube was about 1.5–2.0% resulting in 98% space within the nanotubes bundles. Therefore, we think that this is the major cause responsible for the decaying current response after electrode drying. This compaction reduces interspaces between each bundle resulting in a reduction of the electrochemical active area of the electrode, which is also manifested by the lowering of the current signal with each drying cycle.[18–20]

Further, the shrinkage of the nanotube bundles can also lead to some distortion/modification of the electrode during the process of drying. This modification of electrode might result in the loss of the electrode electrochemical active area. Consequently, the electrode surface can consist of several micron-sized active areas forming a stripe type or disk type microelectrode assembly.[21] This could also account for some reduction of the current response.

The ΔEp value of 140 mV is larger than the ideal value of about 59 mV for a one-electron transfer. This indicates a slower electron transfer rate at the MWNT electrodes than that of the ideal electrode. This is probably due to the slow electron transfer rate at the graphitic basal plane like-MWNTs sidewall.[22] The other reason makes the ΔEp value is higher than 59 mV/1e is the uncompensated iR drop measurement which more resistance in the system can cause the slow electron transfer rate. The stable ΔEp and the linear plot obtained for the peak current versus the square root scan rate indicate a diffusion-controlled, reversible reaction at these electrodes which have faster electron transfer rate than standard glassy carbon electrodes (data not shown).

Note that the electrode response decreases to approximately 4–5 times after drying depending on the electrode original size and becomes stable once the S-shape voltammogram is obtained. Subsequently, the electrode with S-shape voltammogram was applied for electroanalysis. Therefore, the electrode must be dried until the S-shape is obtained before used as an analytical sensor.

3.2. Electrochemical Sensing Properties Evaluation

The stable steady-state voltammetric response obtained for the MWNT electrodes make them suitable for high performance electrochemical sensor materials. For evaluating the electrochemical sensing abilities of these electrodes, a series of model electroactive species, AA and DA were chosen as analytes and tested. Both these species constitutes important intermediates, main products or byproducts in various electrochemical analysis methods. For instance, AA is found extensively in some food products and determining its presence is essential for nutritional evaluations. Similarly, DA is the significant index for Parkinson's disease. Therefore, determining their presence accurately and at very low concentrations becomes crucial for detecting these species.

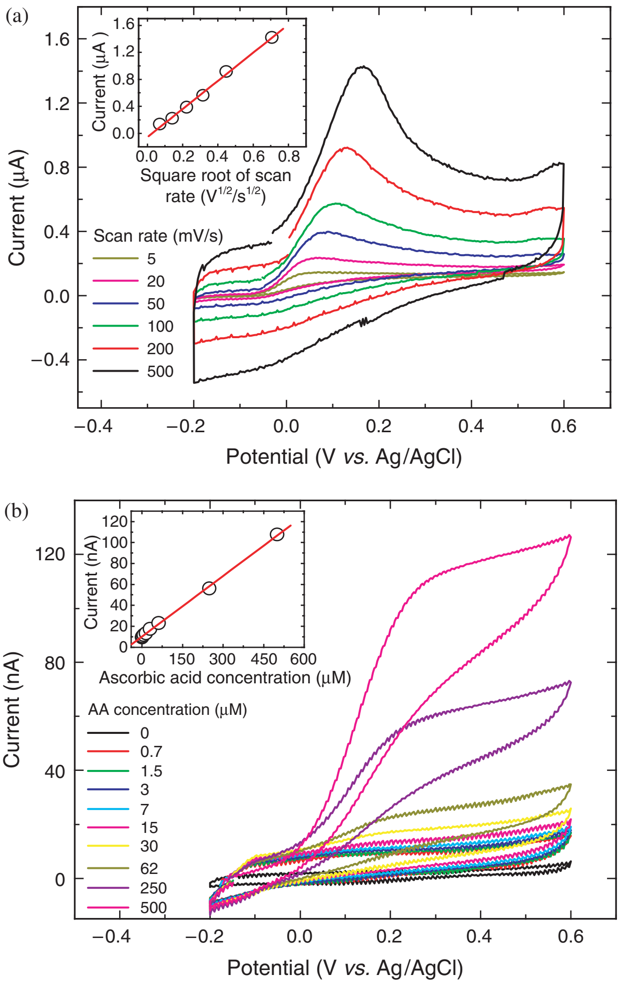

Fig. 3. (a) CVs at MWNT electrode with planar diffusion in 1 mM ascorbic acid (AA) solution containing PBS (pH 7.0) at various scan rate (5, 20, 50, 100, 200, and 500 mV/s) from inner to outer loop respectively. (Inset) A linear plot of current response versus square root of scan rates for 1 mM AA concentration. (b) CVs at MWNT electrode with spherical diffusion in various concentrations of AA (0, 0.7, 1.5, 3.0, 7.0 15.0, 30.0, 62.0, 250 and 500 μM) containing PBS (pH 7.0) at 20 mV/s from inner to outer loop respectively. (Inset) A linear plot of current response versus ascorbic acid concentration.

In case of AA, the oxidation peak was observed at 200 mV without a well-defined reduction peak at 0 mV, suggesting the irreversible nature of the reaction as shown in Figure 3(a). This is due to the inherent instability of the analyte, as reported in some earlier studies.[23, 24] Moreover, the oxidation peak current was found to increase with a negligible shift with the increasing scan rate up to 500 mV/s. The peak current was found to have a linear dependence on the square root of scan rates, with the correlation coefficient of 0.9995 over the range of scan rates (Fig. 3(a) inset). This indicates a diffusion-controlled reaction at the MWNTs electrodes. Figure 3(b) shows an excellent electrocatalytic activity towards the oxidation of AA at these electrodes when the concentration of AA was varied (0, 0.7, 1.5, 3, 7, 15, 30, 62, 250 and 500 μM). Typical electrodes showed a cyclic voltammetry detection limit of as low as 0.7 μM AA concentration. The detection limit of 0.7 μM AA is significantly lower than the detection limit of previously reported carbon nanotubes electrodes[25, 26] as well as other electrode materials.[23, 24, 27–31] The current responses and the concentrations of AA were observed to be linearly dependent represented by the following equation: $y = (1.01) + (0.01)x$ with the correlation coefficient of 0.9993 as shown in Figure 3(b) inset.

In the case of DA very well-defined oxidation and reduction peaks were observed at the potential of about 150 and 139 mV respectively as shown in Figure 4(a) indicating the reversible nature of this reaction at the MWNT electrode. DA concentrations that were easily detected with the MWNT electrode were as low as 1.87 μM. It is

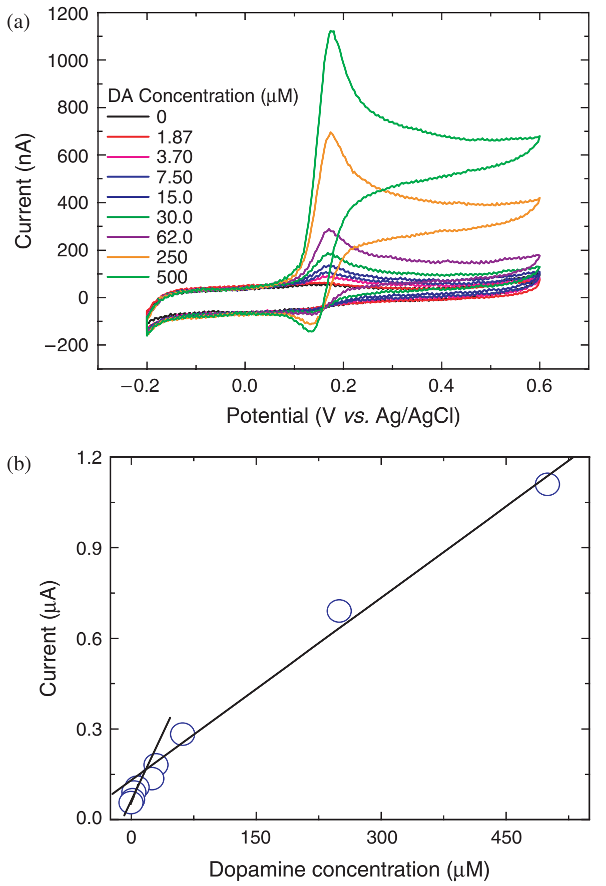

Fig. 4. (a) CVs for the dried-MWNT electrode in various concentrations of dopamine (0, 1.87, 3.7, 7.5, 15, 30, 62, 250 and 500 μM) containing a phosphate buffer solution (pH 7.0) at the scan rate of 20 mV/s. (b) Current response versus dopamine concentration with two intervals linear fit.

worth noting that this detection limit is significantly lower than the detection limit of DNA functionalized CNTs electrodes (0.1 mM) recently reported by Ly.[32] This detection limit is also less than the value reported for some CNTs and other types of electrodes.[33–37] In addition, a non linear current response with increasing DA concentration was observed. This is probably due to the change in the DA mass transport behavior (from adsorption to diffusion) with the increasing concentration.[38]

4. CONCLUSIONS

In summary, ultralong multi-walled microelectrodes were prepared and electrochemically characterized. Steady-state voltammograms were observed at the MWNT electrode at scan rates ranging from 5 to 500 mV/s, with a reversible and a diffusion-controlled reaction. We also tested the electrochemical sensing abilities of these electrodes on two model species, ascorbic acid and dopamine. The results show that these electrodes are superb candidates for single species detection. This suggests that these electrodes will be promising materials for electroanalysis of other electroactive species and can have applications in the filed of chemical and biological sensing.

Acknowledgments: Authors (PMA and RV) acknowledge funding support from the RPI NSF NSEC on directed assembly of nanostructures. NP would like to thank Dr. Mithran Somasundrum for the valuable discussions.

References and Notes

1. Y. Lu, S. Bangsaruntip, X. Wang, L. Zhang, Y. Nishi, and H. Dai, *J. Amer. Chem. Soc.* 128, 3518 (**2006**).
2. R. H. Baughman, A. A. Zakhidov, and W. A. de Heer, *Science* 297, 787 (**2002**).
3. P. Xue, K. H. Park, X. M. Tao, W. Chen, and X. Y. Cheng, *Compos. Struct.* 78, 271 (**2007**).
4. G. Chai and L. Chow, *Carbon* 45, 281 (**2007**).
5. M. Pumera, A. Merkoci, and S. Alegret, *Sens. Actuators B* 113, 617 (**2006**).
6. I. Heller, J. Kong, H. A. Heering, K. A. Williams, S. G. Lemay, and C. Dekker, *Nano Lett.* 5, 137 (**2005**).
7. M. Kaempgen and S. Roth, *Synth. Met.* 152, 353 (**2005**).
8. J. M. Nugent, K. S. V. Santhanam, A. Rubio, and P. M. Ajayan, *Nano Lett.* 1, 87 (**2001**).
9. J. H. T. Luong, S. Hrapovic, D. Wang, F. Bensebaa, and B. Simard, *Electroanalysis* 16 (**2004**).
10. J. H. T. Luong, S. Hrapovic, and D. Wang, *Electroanalysis* 17, 47 (**2005**).
11. R. Antiochia, I. Lavagnini, F. Magno, F. Valentini, and G. Palleschi, *Electroanalysis* 16, 1451 (**2004**).
12. A. Salimi, A. Noorbakhsh, and S. Soltanian, *Electroanalysis* 18, 703 (**2006**).
13. A. Salimi, R. Hallaj, and G. R. Khayatian, *Electroanalysis* 17, 873 (**2005**).
14. J. Heinze, *Ang. Chem. Int. Ed.* 32, 1268 (**1993**).
15. P. Tschuncky and J. Heinze, *Anal. Chem.* 67, 4020 (**1995**).
16. D. O. Wipf and R. M. Wightman, *Anal. Chem.* 60, 2460 (**1998**).
17. Y. Yun, V. Shanov, M. J. Schulz, Z. Dong, A. Jazieh, W. R. Heinemand, H. B. Halsall, D. K. Y. Wong, A. Bange, Y. Tu, and S. Subramaniam, *Sens. Actuators, B* 120, 298 (**2006**).
18. J. Li, A. Cassell, L. Delzeit, J. Han, and M. Meyyappan, *J. Phys. Chem. B* 106, 9299 (**2002**).
19. N. Chakrapani, B. Wei, A. Carrillo, P. M. Ajayan, and R. S. Kane, *PNAS* 101, 4009 (**2004**).
20. P. G. Whitten, G. M. Spinks, and G. G. Wallace, *Carbon* 43, 1891 (**2005**).
21. C. Amatore, J. M. Saveant, and D. Tessier, *J. Electroanalyt. Chem.* 147, 39 (**1983**).
22. R. R. Moore, C. E. Banks, and R. G. Compton, *Anal. Chem.* 76, 2677 (**2004**).
23. F. Wantz, C. E. Banks, and R. G. Compton, *Electroanalysis* 17, 1529 (**2005**).
24. W. Ren, H. Q. Luo, and N. B. Li, *Biosens. Bioelectron.* 21, 1086 (**2006**).
25. J. Fei, Y. Sun, S. Hu, and Z. Gao, *Nanotechnology* 3, 260 (**2004**).
26. L. Jiang, C. Liu, L. Jiang, Z. Peng, and G. Lu, *Anal. Sci.* 20, 1055 (**2004**).
27. Y. X. Sun, S. F. Wang, X. H. Zhang, and Y. F. Huang, *Sens. Actuators, B* 113 156 (**2006**).
28. M. H. P. Azar, H. R. Nerbin, and B. Hafezi, *Electroanalysis* 14, 206 (**2002**).
29. J. B. Raoof, R. Ojani, and A. Kiani, *Electroanalytical Chemistry* 515, 45 (**2001**).

30. R. A. A. Munoz, R. C. Matos, and L. Angnes, *Talanta* 55, 855 (**2001**).

31. R. S. Freire and L. T. Kubota, *Analyst* 127, 1502 (**2002**).

32. S. Y. Ly, *Bioelectrochemistry* 68, 227 (**2006**).

33. H. Boo, R. A. Jeong, S. Park, K. S. Kim, K. H. An, Y. H. Lee, J. H. Han, H. C. Kim, and Chung Taek Dong, *Anal. Chem.* 78, 617 (**2006**).

34. R. K. Shervedani, M. Bagherzadeh, and S. A. Mozaffari, *Sens. Actuators, B* 115, 614 (**2006**).

35. M. Zhang, K. Gong, H. Zhang, and L. Mao, *Biosens. Bioelectron.* 20, 1270 (**2005**).

36. L. Jiang, Q. Xie, Z. Li, Y. Li, and S. Yao, *Sensors* 5, 199 (**2005**).

37. P. J. Britto, K. S. V. Santhanam, and P. M. Ajayan, *Bioelectrochem. Bioenerg.* 41, 121 (**1996**).

38. H. S. Wang, T. H. Li, W. L. Jia, and H. Y. Xu, *Biosens. Bioelectron.* 22, 664 (**2006**).

Received: 19 April 2007. Revised/Accepted: 28 June 2007.